



## Macromolecules cross linked-metal organic frame works based sensors for determination of memantine hydrochloride

Rehab O. El-Attar <sup>a,\*</sup>, Eman M. Shoukry <sup>b</sup>, Eman F. Mohamed <sup>b</sup>, Safaa Omran<sup>b</sup>, Elmorsy Khaled<sup>a</sup>

a) *Microanalysis Laboratory, Applied Organic Chemistry Department, National Research Centre, El Bohouth St., Dokki, 12622 Giza, Egypt*

b) *Department of chemistry, Faculty of Science (Girls), Al Azhar University, Naser City, Egypt*



CrossMark

### Abstract

Fabrication of electrochemical sensors by screen printing technology represents a promising approach for fabrication of a planner electrochemical sensor. Herein, a novel memantine hydrochloride (MEM) potentiometric disposable sensor was constructed based on  $\beta$ -cyclodextrin-metal organic framework-multiwall carbon nanotube composite ( $\beta$ -CD-MOF-MWCNTs) as a selective recognition element for memantine molecule. Improved sensitivity was recorded within the MEM concentration ranged from  $10^{-6}$  to  $10^{-2}$  molL<sup>-1</sup> with a theoretical Nernstian compliance value  $60.5 \pm 0.9$  mV decade<sup>-1</sup> and a limit of detection value of  $7.0 \times 10^{-7}$  molL<sup>-1</sup>. The fabricated disposable sensors showed long shelf lifetime (24 weeks) and fast response time (3s) which may be attributed to the incorporation of covalently bonded ionophore nanocomposite within the electrode matrix. The modified sensors were applied for determination of MEM in biological and pharmaceutical samples with high precision and accuracy. The developed sensors integrated with  $\beta$ -CD-MOF-MWCNTs offer approach for monitoring of the dissolution and degradation studies of memantine.

**Keywords:** Memantine hydrochloride; Screen-printed sensors;  $\beta$ -cyclodextrin-metal organic framework-multiwall carbon nanotube composite; Samples analysis

### 1. Introduction

Memantine hydrochloride (MEM, 1-amino-3, 5-dimethyladamantane) is a non-competitive inhibitor type of the receptor complex, N-methyl-D-aspartate (NMDA). MEM is a common modern therapeutic agent used for treating some diseases such as Alzheimer's disease (AD), glaucoma and stroke. Moreover, MEM is also administrated for the treatment of moderate-to-severe AD, especially for people who are intolerant of or have a contraindication to acetylcholinesterase (AChE) inhibitors [1, 2].

Different analytical approaches were recently reported for monitoring of Alzheimer's disease drugs in their pharmaceutical formulations and biological samples [3]. High performance liquid chromatographic [HPLC] coupled with UV or fluorescence detectors [4-7], RPHPLC [8, 9] or gas chromatography coupled tandem mass spectrometry [10, 11], and capillary zone electrophoretic techniques [12-16] are the most common. Even though the aforementioned analytical approaches offer high sensitivity and selectivity

towards MEM, they are time consuming with several derivatization processes of the samples and operate with high priced instrumentations which are not common in some analytical laboratories.

Electroanalytical methods operate with simple instrumentation equipment with simple pretreatment protocols and short analysis time, and therefore; they were encouraged for monitoring various pharmaceutical compounds [17-20]. Among different electroanalytical techniques, potentiometric sensors are the most common as a simple and sensitive tool for detection of drugs [21-25]. Polyvinylchloride membrane and carbon paste potentiometric sensors have some limitations as short operational lifetimes, complicated fabrication protocol and difficulty to be miniaturized which obstacle their application for analysis of small volume biological samples and other biomedical applications. In recent decades, screen printing technology is sued in a wide range for large-scale production of electrochemical disposable sensors with portable devices [26-32].

Different electrode configurations were reported in literature for potentiometric determination of

\*Corresponding author e-mail: [rhbattar@yahoo.com](mailto:rhbattar@yahoo.com);

Receive Date: 09 September 2023, Revise Date: 01 October 2023, Accept Date: 10 October 2023

DOI: 10.21608/EJCHEM.2023.235254.8579

©2023 National Information and Documentation Center (NIDOC)

memantine in various pharmaceutical formulations and biological fluids. They were based on the integration of the electrode matrix with lipophilic ion-pair complexes of MEM with sodium tetraphenyl borate (TPB), phosphotungstic acid (PTA), tungstosilicic acid (TSA), and ammonium reineckate salt (ARS) [33-35], flavianate (FA), 5-Nitro-barbiturate (NBA) [36], and potassium tetrakis (4-chlorophenylborate [37].

The aforementioned sensors incorporated with ion-pair associates showed limited selectivity and sensitivity and generally not applicable with complex biological samples. Molecular recognition and formation of inclusion complex mechanism offer improvement in the performance of electroanalytical procedures [38-42]. Cyclodextrins (CDs) were the most popular macrocyclic recognition elements for electrochemical sensors. With a lipophobic interior cavity, CDs offer a suitable environment for fitting the nonpolar part of the guest molecule. The stability constants of the formed inclusion complex are governed by the size of both CDs cavity and the guest molecule, the spatial structure of the guest function groups in and the side substitution of the CD ring. [40, 42].

Nanotechnology played an important role for improvement electrochemical sensors performance [43-46]. Nanomaterials have been incorporated within the sensor matrix to promote electrochemical response and prolong the operational lifetime of the sensor. Recently, the progress of crystalline porous materials synthesis has received tremendous attention, where metal-organic frameworks (MOFs) represent a new member in the vast field of porous materials combining the properties of both organic and inorganic porous materials [47, 48]. They are consisting of metal ions with coordination geometry and organic ligands which allowed combining the properties of both organic and inorganic porous materials. The metal ions, organic linkers and structural motifs may yield combinations to form an MOF [49-52]. Postsynthesis modification of MOFs with cyclodextrin macrocyclic compounds assures synergistic performance of both the nanostructure of MOFS and the inclusion complex formation of CDs with the target analyte [53-56]. Therefore, the present work aimed at synthesis and application of novel macrocyclic cross-linked-metal organic with their promising application as molecular recognition element for sensitive and selective determination of memantine potentiometrically in biological fluids and pharmaceutical formulations.

## 2. Experimental

### 2.1. Chemicals and reagents

All chemicals and reagents were of analytical grade. Different types of molecular

recognition ionophores were utilized as electroactive sensing elements including:  $\alpha$ - (I),  $\gamma$ - (II),  $\beta$ -CD (III, Sigma), heptakis (2,6-di-O-methyl)-  $\beta$ -CD (IV, Aldrich), heptakis (2,3,6-tri-O-methyl)- $\beta$ -CD (V, Aldrich), 12-crown-4 ether (VI, Fluka), 15-crown-5 ether (VII, Fluka), 18-crown-6 ether (VIII, Fluka), 21-crown-7 ether (IX, Fluka), dibenzo 24-crown-8 ether (X, Fluka), 30-crown-10 ether (XI, Fluka), calix[4]arene (XII, Aldrich), and calix[8]arene (XIII, Aldrich).

The following tetraphenylborate derivatives were used as ionic sites including; sodium tetraphenylborate (NaTPB, Fluka), sodium tetrakis (4-fluorophenyl) borate (NaTFPB, Fluka), and potassium tetrakis (4-chlorophenyl) borate (KTCIPB, Fluka). Some membrane plasticizers types with different dielectrical constants were used such as 2-fluorophenyl-2-nitrophenyl ether (*f*-PNPE, Fluka), *o*-nitro-phenyloctylether (*o*-NPOE, Sigma), tricresylphosphate (TCP, Fluka), dioctylsebacate (DOS, Avocado) and dioctylphthalate (DOP, Sigma).

Polyvinyl chloride (PVC, Aldrich), and graphite powder (synthetic 1-2  $\mu$ m, Aldrich), were used for synthesis of the printing inks preparation, graphene nano sheet (Gr, Sigma), single wall nanotubes (SWCNTs, Aldrich) and multiwall nanotubes (MWCNTs, Aldrich) were used for composite synthesis. Solutions of the interferents were prepared such as:  $\text{Li}^+$ ,  $\text{Ca}^{+2}$ ,  $\text{Co}^{+2}$ ,  $\text{Mg}^{+2}$ ,  $\text{NH}_4^+$ ,  $\text{Ni}^{+2}$ , starch, glucose, maltose, sucrose, fructose phosphate, citrate, caffeine cysteine and glycine.

### 2.2. Authentic samples

Memantine hydrochloride standard sample (MEM,  $\text{C}_{12}\text{H}_{22}\text{ClN}$ ,  $215.76 \text{ g mol}^{-1}$ ) was kindly supplied by the Arab Drug Company (ADCo, Cairo, Egypt). The standard MEM solution ( $1 \times 10^{-2} \text{ mol L}^{-1}$ ) was prepared by dissolving the appropriate weight of MEM in bidistilled water. Other working MEM solutions were prepared by serial dilution of the stock MEM solution.

### 2.3. Pharmaceutical and biological samples

Memantine pharmaceutical sample (Ebixa®, Rottendorf Pharma GmbH – Germany, assigned to contain 10 mg MEM/tab) were purchased from local drug stores. Ten tablets were weighed, grinded to fine powder, and a quantity equal one tablet was dissolved in bidistilled water, filtered off and analyzed according to the official method in comparison with the proposed potentiometric approach.

Standard plasma samples (VACSERA, Dokki, Giza), were fortified with known aliquots of the MEM stock standard solution, vortexed with acetonitrile, and centrifuged at 10000 rpm for 10 min at 4°C to get rid of the protein. Urine samples were laced with aliquots of the standard MEM solution, treated with methanol to remove protein and the MEM contents in both clear supernatants were

analyzed potentiometrically and according to the pharmacopeial protocol.

#### 2.4. Apparatus

A portable 46-Range Digital Multimeter (Radioshack, China) with a PC interface was used for potentiometric measurements. The pH of the measuring electrolyte was adjusted using a 692-pH meter (Metrohm, Herisau, Switzerland). Manual screen printer (China) was used for printing of electrodes on PVC sheet through a patterned stainless steel stencil (200  $\mu\text{m}$  thickness) with six rectangular openings of dimensions 5 $\times$ 35 mm. An ultrasonic water bath J.P. Selecta, Ultrasons (Spain) was used for achieving complete solubility, homogeneity and getting rid of air bubbles of the prepared solutions and inks.

#### 2.5. Synthesis of MIL-53-NH<sub>2</sub>-cross-linked macromolecule composites

Selected cyclic macromolecules were linked with the functionalized metal organic framework including;  $\beta$ -cyclodextrin (**III**), 18-crown-6 ether (**VIII**), and calix[8] arene (**XIII**). MIL-53(Al)-NH<sub>2</sub> was first synthesized by mixing 2-aminobenzenedicarboxylic acid and AlCl<sub>3</sub>.6H<sub>2</sub>O solution at room temperature in a 40 mL Teflon®-lined stainless steel bomb. For complete growth of the framework, then heated at 110 °C for 24 hours. The resultant precipitate was cleaned at 160°C with water and DMF, and then it was soaked in CH<sub>2</sub>Cl<sub>2</sub> for 24 hours before being dried in the air at 80°C. The cross-linked MIL-53-NH<sub>2</sub>-cross linked macromolecule composites were synthesized and characterized as described in details elsewhere [57, 58].

#### 2.6. Construction of MEM disposable sensors

The disposable sensors were printed on a PVC sheet using graphite-based and silver-silver chloride based inks for working and reference electrodes, respectively [59]. The membrane matrix cocktail was prepared by dissolving 1.0 mg of the MIL-53(Al)-NH<sub>2</sub>- $\beta$ -CD nanocomposite, 0.5 mg NaTFPB in 360 mg *o*-PNPE. After stirring for 15 min, 6 mL tetrahydrofuran was added with sonication for 2 h followed by addition 240 mg PVC and 15.0 mg MWCNTs. Further sonication was carried out for extra 30 min to ensure complete homogeneity, and the result matrix was printed on the surface of the graphite/PVC conducting track. After drying for 24 h at 50 °C, the constructed sensors were directly used after preconditioning for 5 min in 10<sup>-3</sup> molL<sup>-1</sup> MEM solution.

#### 2.7. Calibration of sensor

The modified sensors were calibrated for batch measurements by immersing the sensor in MEM solutions covering the concentration range from 10<sup>-7</sup> to 10<sup>-2</sup> mol L<sup>-1</sup>. The potential readings were plotted against logarithmic scale of drug concentration [60].

#### 2.8. Memantine tablet dissolution profile

Ebixa tablet was put in the dissolution vessel containing 50 mL HCl solution (10<sup>-1</sup> mol L<sup>-1</sup>, pH 1.2) at 37 $\pm$ 0.5 °C with rotation speed 50 rpm [61]. After specific intervals, 4 mL were withdrawn from the sample and the amount of MEM released in the dissolution medium was measured using the modified MEM-potentiometric methods and UV spectrophotometric measurements at 254 nm [12].

#### 2.9. Forced degradation studies

Under suitable conditions, forced degradation of MEM was carried out using standard material [62]. MEM was dissolved in 10% H<sub>2</sub>O<sub>2</sub>, 0.1 M HCl/NaOH solutions and incubated at 70 °C. The degradation process was followed spectrophotometrically at 254 nm, and at the end of degradation process, solutions were neutralized and analyzed according to the recommended procedures.

20 tablets of MEM were exposed drying at heat (105°C) for 5 days in an oven under temperature stress. The tablets were grinded and mixed in a mortar and pestle. The appropriate weight was used for analysis using the developed analytical method in comparison with the spectrophotometric ones.

### 3. Results and discussion

#### 3.1. Optimization of the sensing matrix compositions

It is well-known that macrocyclic compounds can host a variety of guests within their cavities. The adamantyl group is one of the most suitable guest molecules that can be accommodated by cyclodextrin with a diameter that is suitable and fits well into the cyclodextrin cavity. Based on the formation of such inclusion complex, cyclodextrin and other macrocyclic compounds including crown ethers, calixarenes, and their nanocomposites with metal organic frameworks can be introduced as sensing materials for potentiometric determination of memantine in authentic and pharmaceutical formulation samples.

Parallel and comprehensive studies were performed to achieve the highest sensor performance through investigation of the impact of the type and concentration of sensing material, hydrophilic additives, membrane plasticizer and nature of nanomaterials.

##### 3.1.1. Nature of the sensing material

Sensor matrices were incorporated with different free macrocyclic compounds (cyclodextrins, crown ethers, and calixarenes (**I-XIII**)). In the absence of the sensing elements, the dummy electrodes contained only NaTPB as ionic sites, showed sub-Nernstian slope (42.2  $\pm$  2.2 mV decade<sup>-1</sup>), while in the presence of different macrocyclic molecules, improved potentiometric responses were recorded (**Figure 1**).

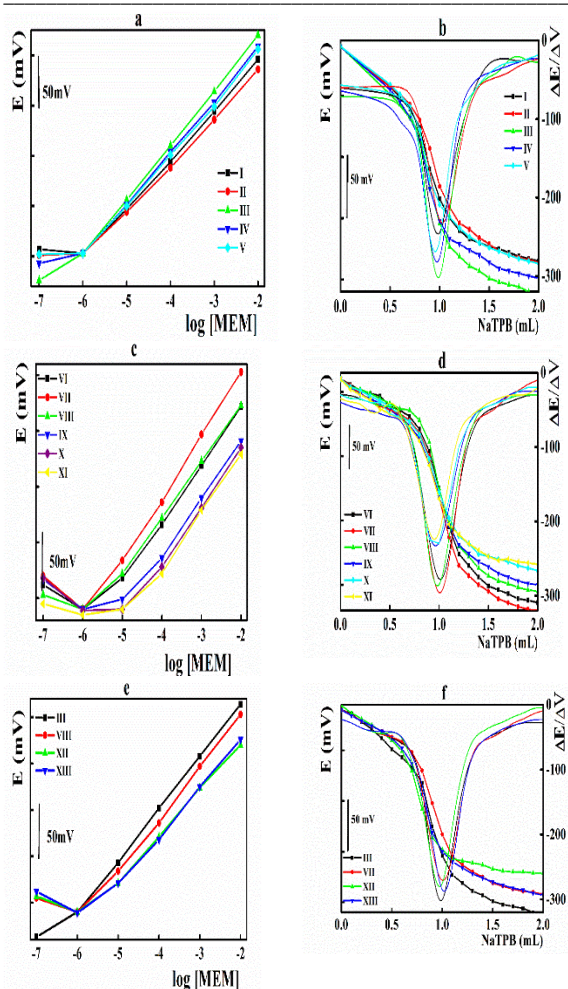


**Figure 1: Impact of the sensing material on: a, c, e) performance of MEM sensor; b, d, f) potentiometric titration against NaTPB solution.**

Preliminary, successive measurements indicate gathering of the Nernstian slopes in the first calibration followed by decreasing in the subsequent ones until no electrode response was obtained. Therefore, more attention must be given to the selection of sensing materials with multiple calibration curves.

Among different cyclodextrin derivatives, the native  $\beta$ -CD (**III**) showed the proper performance with Nernstian slope value  $54.2 \pm 0.3$  mV decade<sup>-1</sup> in the MEM linear concentration range from  $10^{-6}$  to  $10^{-2}$  mol L<sup>-1</sup> (**Figure 1a**). Contrary, both  $\alpha$ - and  $\gamma$ -CD (**I**, **II**) showed lower Nernstian response ( $48.3 \pm 0.9$  and  $45.8 \pm 0.8$  mV decade<sup>-1</sup>, respectively) based on their improper cavity size and lower stability of the formed CD-MEM inclusion complexes. On the other hand, side derivatization of the cyclodextrin ring with the methyl groups (**IV**, **V**) showed slightly lower Nernstian response based on the steric hindrance caused by the side methyl group arms which effect

the inclusion complex formation. Performing the potentiometric titration of the target analyte (MEM) against NaTPB (**Figure 1 b**), similar trend was recorded as the native  $\beta$ -CD (**III**) exhibited the highest potential jump (202 mV) and  $\Delta E/\Delta V$  ( $360$  mV mL<sup>-1</sup> titrant).

Alternatively, crown ethers recorded different Nernstian slope values governed by their cavity size capable to fit the adamantyl group of MEM molecule (**Figure 1c & d**). Among them, 15-crown-5 ether (**VII**) showed the highest Nernstian slope value ( $56.8 \pm 1.1$  mV decade<sup>-1</sup> within the MEM concentration ranged from  $10^{-5}$  to  $10^{-2}$  mol L<sup>-1</sup>), compared with other tested crown ethers.

Finally, sensors performances incorporated with the selected  $\beta$ -CD derivative (**III**), and crown ether (**VII**) were compared with those containing calix [4] arene (**XII**) and calix [8] arene (**XIII**) (**Figure 1e & f**). Results indicated the superiority  $\beta$ -CD (**III**) as the highest sensor performance compared with the other testing ionophores under either direct potentiometric or potentiometric titration measurements.

Moreover, the  $\beta$ -CD (**III**) content within the electrode matrix was varied from 0.0 to 5.0 mg. Nernstian slope ( $42.2 \pm 2.2$  mV decade<sup>-1</sup>) was recorded for the dummy membrane sensor, while the presence of 1.0 mg of  $\beta$ -CD, improved sensor performance was obtained ( $51.5 \pm 0.3$  mV decade<sup>-1</sup>). At higher ionophore concentrations gave lower Nernstian slope ( $48.8 \pm 0.9$  mV decade<sup>-1</sup> for 5.0 mg) was recorded due to over saturation of the electrode membrane matrix.

Next, the selected aforementioned sensing elements were cross-linked with MIL-53-NH<sub>2</sub> metal organic frameworks, and the resulting nanocomposites were incorporated within the electrode matrix instead of the corresponding free ionophores (**Figure 2**). The characteristic performances of the constructed sensors indicated noticeable enhancement of the Nernstian slope value upon complexation of the sensing ionophore with the MOF structure which can be explained on the base of enhanced electroactive surface area and increasing the complexation sites with MEM molecule. Among the tested sensors, integration of the electrode matrix with  $\beta$ -CD-MOF composite showed the highest sensitivity under direct potentiometric measurements and potentiometric titration conditions as in (**Figure 2 a, b**).



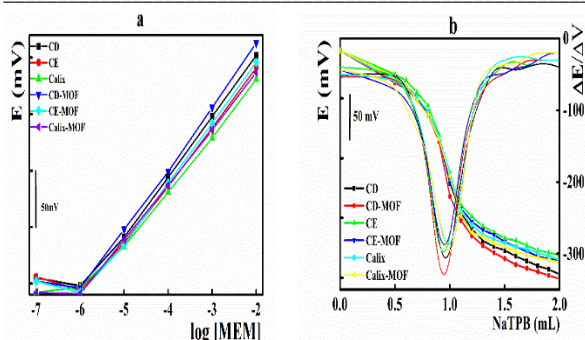


**Figure 2:** Effect of the cross-linking with metal organic frameworks on: a) performance of MEM sensor; b) potentiometric titration against NaTPB solution.

Carbonaceous nanomaterials with their unique features promote enhances and stimulate transduction of the signal from chemical to electrical within the sensor matrix, which in turn improve the sensor performance [43-46]. The printed sensors integrated with either the free  $\beta$ -CD or  $\beta$ -CD-MOF composite were evaluated in the presence of different carbonaceous nanomaterials including graphene nano sheet (rG), multiwall nanotubes (MWCNTs), and single wall nanotubes (SWCNTs). Incorporation of MWCNTs improved the sensors performance with the highest Nernstian slope value of  $59.9 \pm 0.8$  mV decade<sup>-1</sup> for  $\beta$ -CD-MOF-MWCNTs based sensors (Figure 3 a). In addition, under potentiometric titration conditions,  $\beta$ -CD-MOF-MWCNTs showed the highest potential jump was ( $\Delta E=216$  mV) and potential break at the end point (Figure 3 b).

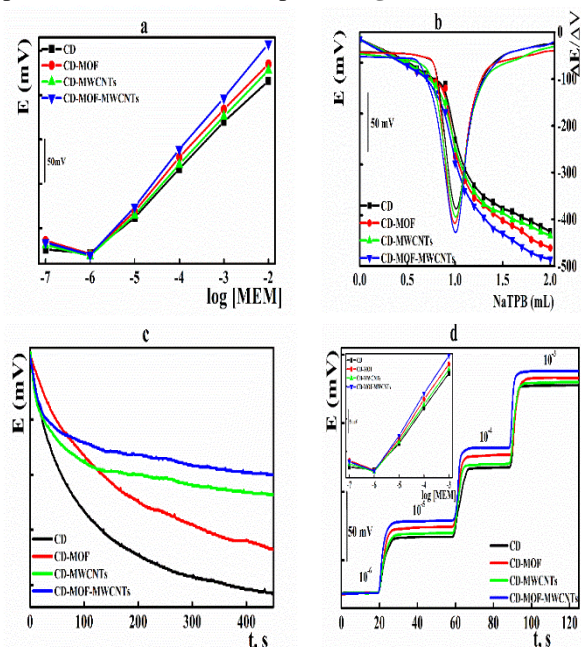


**Figure 3:** Effect of the sensing nanomaterials on: a) performance of MEM sensor; b) potentiometric titration against NaTPB solution; c) preconditioning time; e) electrode response time.

Following the sensor fabrication protocol, screen printed sensors required short preconditioning time compared with other solid contact electrodes (coated wires and coated graphite). This can be explained on the basis of co-polymerization of the sensing membrane matrix with the conducting carbon track matrix which obstacle the formation of the undefined water layer between the sensing membrane and conducting carbon track. The incorporation of nanomaterials showed an additional enhancement of the sensor potential stability due to their high surface area, enhancement of the hydrophobicity of the sensing membrane surface, which contributes to the more stable potential signal. Sensors integrated with MWCNTs achieved potential stability reading within very short preconditioning time (less than 5 min) compared with the corresponding carbon

The impact of the nanomaterial on the electrode dynamic response time (the time required by electrode to achieve 90% of the total potential change after sudden tenfold increase in the analyte concentration) was monitored within MEM concentration ranged from  $1 \times 10^{-6}$  to  $1 \times 10^{-3}$  mol L<sup>-1</sup>. Fast response time (about 3 s) was estimated for  $\beta$ -CD-MOF-MWCNTs which may be attributed to their high surface area which improves the matrix conductivity and transduction of the chemical signal to electrical signal (Figure 3d).

### 3.1.2. Ionic sites effect

As a neutral carrier ionophore; potentiometric sensors based on CD operate only when ionic sites are present in the sensing membrane matrix. Ionic sites with opposite charge to the target analyte, attract the drug molecule to the electrode surface and enhance the ion exchange kinetics at the sensing membrane surface [63-65]. Herein, sensors containing  $\beta$ -CD-MOF-MWCNTs as a sensing element were incorporated with different tetraphenylborate derivatives as anionic sites (Figure 4a). Different Nernstian slope values were recorded;  $30.8 \pm 0.5$ ,  $54.8 \pm 0.7$ ,  $57.0 \pm 1.1$  and  $59.6 \pm 0.4$  mV decade<sup>-1</sup> for the blank, NaTPB, NaTFPB and KTCIPB based sensors, respectively. Moreover, performing potentiometric titration applying sensors containing different anionic sites (Figure 4b) sustained this concept as the highest potential jump was recorded applying NaTFPB with ( $\Delta E=217$  mV;  $\Delta E/\Delta V=740$  mV mL<sup>-1</sup> titrant).

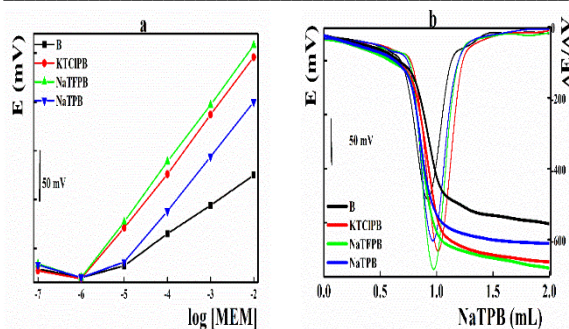


**Figure 4:** Impact of the ionic sites on: a) performance of MEM sensor; b) MEM potentiometric titration & NaTPB solution

Next, the content of NaTFPB was studied from 0.0 to 3.0 mg. Nernstian responses give the highest potential when we use 1.0 mg of NaTFPB.

### 3.1.3. Membrane plasticizer effect

The performance of the molecular recognition-based sensors is mainly governed by the sensing membrane polarity which effects on the mobility of molecular recognition element and their formed inclusion complexes [65-67]. Five plasticizers having different dielectric constants were included namely: DOP, DOS, TCP, *o*-NPOE, and *f*-PNPE ( $\epsilon=3.8, 5.2, 17.6, 24,$  and  $50,$  respectively) [68]. Electrodes containing high polar plasticizers showed improved Nernstian slope values ( $60.5\pm 0.9$  and  $59.6\pm 0.4$  mV decade<sup>-1</sup> for *f*-PNPE and *o*-NPOE, respectively) compared with tested plasticizers (Figure 5a).

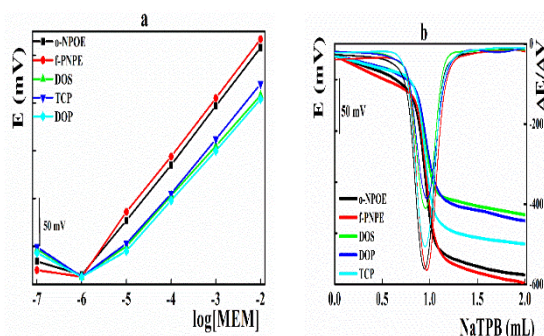


**Figure 5:** Effect of the membrane plasticizer on: a) performance of MEM sensor; b) potentiometric titration against NaTPB solution

Also, potentiometric titration of MEM against NaTPB as titrant was performed with sensors incorporated with the cited plasticizers (Figure 5 b). Both *f*-PNPE and *o*-NPOE showed the highest potential jump based on their polarity and dielectrical constants (potential jump values were 121, 155, 188,

214 and 222 mV for DOP, DOS, TCP, *o*-NPOE and *f*-PNPE, respectively).

### 3.2. Sensor performance

According to the IUPAC recommendation, the performance characteristics of the different fabricated disposable sensors integrated with  $\beta$ -CD-MOF-MWCNTs nanocomposite as molecular recognition element was validated against memantine (Table 1) [60]. The developed sensors showed Nernstian slope of  $60.5\pm 0.9$  mV decade<sup>-1</sup>, and detection limit  $8\times 10^{-7}$  molL<sup>-1</sup>.

**Table 1:** Analytical parameters of modified MEM screen printed sensors screen printed sensors

Sensor	$\beta$ -CD	$\beta$ -CD-MOF	$\beta$ -CD-MOF-MWCNTs
Concentration range (molL <sup>-1</sup> )	$10^{-5}$ - $10^{-2}$	$10^{-6}$ - $10^{-2}$	$10^{-6}$ - $10^{-2}$
Slope (mV decade <sup>-1</sup> )	$51.5\pm 1.0$	$54.3\pm 0.3$	$60.5\pm 0.9$
R	0.9992	0.9990	0.9994
LOD (molL <sup>-1</sup> )	$1.0\times 10^{-6}$	$1.0\times 10^{-7}$	$7.0\times 10^{-7}$
Response time (s)	10	8	3
Preconditioning time (min)	10	10	5
Shelf-life time (week)	4	12	24

With high fabrication reproducibility, the average Nernstian slope values for ten printed electrodes were  $59.7\pm 1.1$  mV decade<sup>-1</sup> with standard potential ( $E^0$ )  $352.5\pm 3.3$  mV. Due to the absence of internal reference solution, the developed MEM disposable sensors showed all solid-state nature, therefore, they show prolonged shelf lifetime for 24 weeks during which the recorded Nernstian slopes did not significantly changed. Moreover, the same fabricated disposable sensors can operate contentiously up to more than 2 months without diminishing of their performance.

The performance of the proposed MEM sensor integrated with  $\beta$ -CD-MOF-MWCNTs nanocomposite was compared with the previously reported memantine sensors [33-37]. The presented sensors offer enhanced performance regarding the linear range, detection limit, and fast response time compared with other MEM reported sensors (Table 2). Moreover, as the introduced sensors are disposable, no preconditioning time was required with the advantages of low-cost mass production of the sensors.

For appropriate application of a newly developed potentiometric sensors, the working pH

range is one of the crucial operating factors. Herein, the electrode response was monitored at different pH values ranged from 2 to 10 (Figure 6). Stable and reproducible response was recorded with a wide pH range from 4 to 10 allowing analysis of different

pharmaceutical and biological samples without the requirement of pretreatment steps. Above pH 10, the electrode potential decreased due to formation of the deprotonated species (pKa is 10.42) and precipitation of MEM base.

**Table 2: Comparison of the electroanalytical performances for different memantine sensors**

Sensors	Present	33	34	35	36	37
Type of sensor	SPE	PVC	PVC	CPE	PVC	Pt/Au
Electroactive material	$\beta$ -CD-MOF-MWCNTs	MEM-NaTPB	MEM-TPB MEM-ARS	MEM-IPs	MEM-FA MEM-PMA	KTCIPB
Linear range (molL <sup>-1</sup> )	10 <sup>-6</sup> -10 <sup>-2</sup>	10 <sup>-5</sup> -10 <sup>-2</sup>	10 <sup>-4</sup> -10 <sup>-1</sup>	10 <sup>-6</sup> -10 <sup>-2</sup>	5×10 <sup>-5</sup> -10 <sup>-2</sup>	10 <sup>-5</sup> -10 <sup>-2</sup>
Slope (mV decade <sup>-1</sup> )	60.5±0.9	59.7	59.34	57.8±0.4	55.45	58.5 ± 1
LOD (molL <sup>-1</sup> )	7.0×10 <sup>-7</sup>	9.0×10 <sup>-6</sup>	-----	7.0×10 <sup>-7</sup>	1.74×10 <sup>-6</sup>	2.5 × 10 <sup>-6</sup>
Titration range (mg)	1.79-8.95	-----	-----	-----	-----	-----
Response time (s)	3	25	10	10	10	≤10
Preconditioning Time	5 min	24 h	24 h	60 min	120 min	60 min
Shelf-life time (week)	24	4-10	4	----	-----	-----
Working pH range	4-10	5-8.5	2-8	2-8	2.66-9.54	3-8
Degradation studies	Done	-----	-----	-----	Done	-----
Dissolution studies	Done	----	----	----	Done	-----

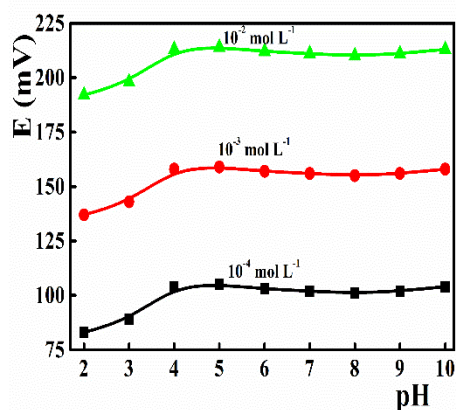


**Figure 6: Potentiometric response of the fabricated memantine sensors at different pH values**

**3.3. Sensor selectivity and degradation studies**

For a newly developed analytical approach, the selectivity towards the target analyte is a crucial issue. For potentiometric sensors, the term selectivity was used to describe the ability of the sensors to differentiate interfering species about target analyte and expressed by selectivity coefficient [69]. For neutral species, the matched potential (MPM) method was recommended [70, 71]. Herein, the selectivity of the introduced sensor towards MEM was tested in the

presence of additives and excipients that usually present in the pharmaceutical formulation (Table 3). The fabricated sensors integrated with  $\beta$ -CD-MOF-MWCNTs nanocomposite showed enhanced selectivity which may be attributed to the inclusion complex formation between the target analyte (MEM) and cyclodextrin moiety within the nanocomposite structure.

**Table3: Selectivity coefficients of the fabricated memantine sensors**

Interferent	-log K <sub>A,B</sub>	Interferent	-log K <sub>A,B</sub>
Li <sup>+</sup>	3.80	Maltose	3.90
NH <sub>4</sub> <sup>+</sup>	3.40	Starch	3.74
Ca <sup>2+</sup>	3.10	Sucrose	3.60
Mg <sup>2+</sup>	3.44	Glucose	3.29
Ni <sup>2+</sup>	3.90	Fructose	3.35
Co <sup>2+</sup>	3.53	Glycine	2.85
Phosphate	3.70	Caffeine	3.40
Citrate	2.54	Cysteine	2.80

Degradation profiling of a pharmaceutical product means the monitoring and quantifying of the various degradants in bulk materials and in the final pharmaceutical formulations during its shelf lifetime. Monitoring and quantification of such contaminants is one of the most crucial considerations in the modern pharmaceutical industry as recommended by the ICH Guideline [72, 73]. Some of such degradants may be health hazards, therefore, monitoring of such



impurities should be taken in consideration to ensure the safety of the final pharmaceutical product [73-75].

In the present study, MEM was degraded under hydrolytic and forced degradation conditions [76]. More than 18 and 13% of the original MEM were degraded after 1 h in an acidic medium and alkaline medium, respectively, while complete degradation was recorded after 3 h. Negligible amounts (4, <2%) were degraded under oxidative, thermal, and photolytic degradation of MEM. The aforementioned degradation and interference studies devoted the application of the potentiometric approach for selective quantification of memantine in the pharmaceutical formulation as stability indicating protocol without the necessity of pretreatment or separations steps.

### 3.4. Analytical applications

#### 3.4.1. Potentiometric titration

Potentiometric measurements under direct potentiometric conditions required tedious and careful calibrations of the measuring cells. On the other hand, potentiometric titration offers the advantage of high accuracy and precision; in spite of the cost of increased time and consumption of reagents [77]. The fabricated disposable sensors incorporated with  $\beta$ -CD-MOF-MWCNTs showed symmetrical titration curves with high potential jump ( $\Delta E$  ranged from 183 to 235 mV for 1.79 to 8.95 mg MEM) and potential breaks at the inflection point about 400 mV mL<sup>-1</sup> (Figure 7 a). Titration process was highly producible as performing titration of 1.79 mg MEM showed total average recovery value of 100.5 $\pm$ 2.51% (Figure 7b).

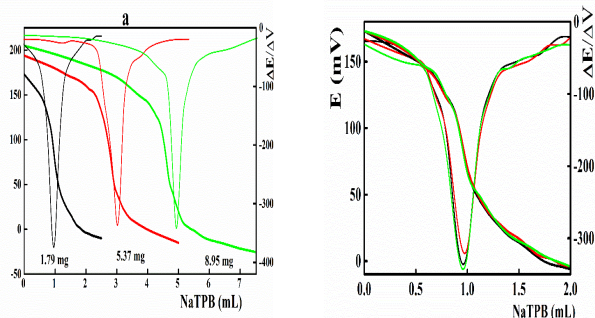


**Figure 7:** a) Potentiometric titration memantine against NaTPB using  $\beta$ -CD-MOF-MWCNTs integrated sensors, b) reproducibility of titration for 1.79 mg MEM.

#### 3.4.2. Sample analysis

Memantine undergoes little metabolism after oral administration and converted to three simple metabolites: 6-hydroxy memantine, N-gludantan conjugate and 1-nitroso-deaminated memantine [78]. The percentages of metabolites were 68.7% for the

parent memantine, 12.9% for the N-gludantan conjugate, 6.51% for the 6-OH metabolite, and 5.87% for the 1-nitroso-deaminated memantine. Based on the molecular structure of the aforementioned metabolites, it is expected that only the 6-OH metabolite has closely the chemical structure of the parent memantine compound and can interfere in its potentiometric assay.

Based on the recorded satisfactory selectivity and sensitivity of the developed MEM sensors, they can be advised for the routine quality control analysis of memantine in pharmaceutical formulations and biological fluids under direct potentiometric measurements and potentiometric titration modes. Satisfactory agreement between the drug contents in various samples determined by the developed sensor and official methods (Table 4).

#### 3.4.3. Dissolution Test

After oral drug administration, the release and absorption of pharmaceutically active compound in a solid dosage represents a crucial factor to explain pharmacokinetics behavior of the drug. Moreover, the dissolution testing is usually relevant to predict performance in vivo and suggest new formulations that might have slower or faster release according to the pharmaceutical compound use.

Recently, potentiometric sensors were introduced as an efficient tool for the in-line dissolution profiling of many pharmaceutical compounds [79-81]. In the present study, the dissolution profile and the release of MEM in Ebixa® tablet was monitored with the fabricated MEM sensor and the UV-spectrophotometric measurement at 254 nm. After each 2 min time intervals, aliquots were continuously withdrawn and the MEM content was assayed potentiometrically from the calibration curve and compared with the UV measurements. Results illustrated in (Figure 8) showed that both of two methods have closed agreements in recoveries about  $\pm$ 2.0%. More than 90 % memantine hydrochloride amount was released within 10 min and the completed hydrolysis was found after 15 min.

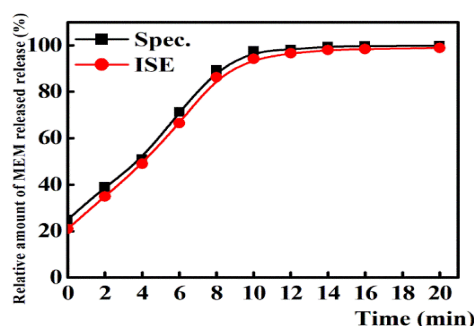


**Figure 8:** Dissolution profile of memantine from Ebixa tablet (10 mg MEM/tablet) using proposed potentiometric and spectrophotometric method.



**Conclusion**

The developed method demonstrates the fabrication and electroanalytical performance of a novel memantine disposable potentiometric sensors based on  $\beta$ -cyclodextrin cross-linked metal organic framework-multiwall carbon nanotube composite as molecular recognition element. The introduced sensors showed Nernstian compliance  $60.5 \pm 0.9$  mVdecade<sup>-1</sup> within the linear concentration range

from  $10^{-6}$  to  $10^{-2}$  mol L<sup>-1</sup> and short response time (3s) with long lifetime up to 24 weeks. The presented sensors showed improved electroanalytical characteristics compared with the previously reported MEM sensors. The proposed sensors were successfully applied for quantification of memantine in biological fluids and pharmaceutical samples in the coexistence of interferants and degradation products.

**Table 4: Potentiometric quantification of memantine in biological and pharmaceutical samples**

Sample	Taken ( $\mu\text{g}$ )	Ebixa®			Spiked Urine			Spiked Plasma		
		Found ( $\mu\text{g}$ )	Recovery	RS D	Found ( $\mu\text{g}$ )	Recovery	RS D	Found ( $\mu\text{g}$ )	Recovery	RSD
Standard addition	1.79	1.81	101.3	1.7	1.72	96.3	2.4	1.73	96.9	2.9
	17.90	17.63	98.5	1.2	17.51	97.8	1.9	17.38	97.1	2.3
	179.00	176.5	98.6	1.9	177.0	98.9	1.4	176.85	98.8	1.9
Titration	1790.0	1750.6	97.8	1.4	1782.8	99.6	1.1	1793.6	100.2	1.35
	1790	1743.5	97.4	2.4	1707.7	95.4	3.1	1677.2	93.7	3.6
	5370	5310.9	98.9	2.0	5208.9	97.6	2.7	5074.6	94.5	3.1
	8950	8976.8	100.3	1.5	8878.4	99.2	1.8	8645.7	96.6	2.1

<sup>a</sup> Mean recovery and five determinations for relative standard deviations

**Conflicts of interest**

"There are no conflicts to declare".

**Formatting of funding sources**

No foundation sources

**Acknowledgments**

"The authors thankfully acknowledge Prof. Dr. Reda M. Abdelhameed for synthesis and supplying with the metal organic frame works"

**References**

1. Mount C. D., and Wnton C., Alzheimer disease: progress or profit?". *Nature Medicine*, **12** (7), 780–784 (2006).
2. NICE review of technology appraisal guidance 111 January 18 (2011).
3. Erkmen, C., Bozal - Palabiyik, B. and Uslu B., Overview of Analytical Methods in Alzheimer's disease Drugs: Optical, Chromatographic, and Electrochemical Methods. *Frontiers in Clinical Drug Research-Dementia*, **1**, 132-164 (2020).
4. Shuangjin, C., Fang, F., Han, L. and Ming, M., New method for high-performance liquid chromatographic determination of amantadine and its analogues in rat plasma. *Journal of pharmaceutical and biomedical analysis*, **44** (5), 1100-1105 (2007).
5. Narola, B., Singh, A.S., Santhakumar, P.R. and Chandrashekhar, T.G., A validated stability-indicating reverse phase HPLC assay method for the determination of memantine hydrochloride drug substance with UV-detection using pre column derivatization technique. *Analytical chemistry insights*, **5**, 37-45 (2010).
6. Puente, B., Garcia, M.A., Hernandez, E., Bregante, M.A., Perez, S., Pablo, L. and Prieto, E., Determination of memantine in plasma and vitreous humour by HPLC with pre column derivatization and fluorescence detection. *Journal of chromatographic science*, **49** (10), 745-752 (2011).
7. Hassan, M.G., Emara, K.M., Mohamed, H.A., Abdel-Wadood, H.M., Ikeda, R., Wada, M., Kuroda, N. and Nakashima, K., Determination of memantine in rat plasma by HPLC-fluorescence method and its application to study of the pharmacokinetic interaction between memantine and methazolamide. *Biomedical Chromatography*, **26** (2), 214-219 (2012).
8. Thangabalan, B., Sandhya, C., Sunitha, N. and Babu, S.M., Stability Indicating RP-HPLC Method for the Estimation of Memantine Hydrochloride in Pure and Pharmaceutical Dosage Form. *Research Journal of Pharmaceutical Dosage Forms and Technology*, **5** (6), 334-340 (2013).
9. Anees, A., Bahazeq, A.A., Rehman, M.U., Akbar, S. and Mehveen, J., Development and validation of memantine hydrochloride by RP-HPLC method. *Asian Journal of Pharmaceutical Research*, **9** (2), 69-74 (2019).
10. Almeida, A.A., Campos, D.R., Bernasconi, G., Calafatti, S., Barros, F.A.P., Eberlin, M.N., Meurer, E.C., Paris, E.G. and Pedrazzoli, J., 2007. Determination of memantine in human plasma by liquid

- chromatography–electrospray tandem mass spectrometry: Application to a bioequivalence study. *Journal of Chromatography B*, **848** (2), 311-316 (2007).
11. Tsuruoka, Y., Nakajima, T., Kanda, M., Hayashi, H., Matsushima, Y., Yoshikawa, S., Nagata, M., Koike, H., Nagano, C., Sekimura, K. and Hashimoto, T., Simultaneous determination of amantadine, rimantadine, and memantine in processed products, chicken tissues, and eggs by liquid chromatography with tandem mass spectrometry. *Journal of Chromatography B*, **1044**, 142-148 (2017).
  12. Bahazeq, A.A., Syeda, W.N., Isba, N.F., Rehman, M. and Baqi, U.A., Assay of memantine hydrochloride by UV spectrophotometer. *Int J Pharm Sci Res*, **10** (1), pp.27-30 (2019).
  13. Navneet, K., Karan, M., Rishabh, N., Ashutosh, U., Kunal, N. and Arti, T., Estimation of memantine hydrochloride using ultraviolet-visible spectrophotometry in bulk drug and formulation. *Journal of Pharmaceutical Research*, **10**(2), 80-82 (2011).
  14. Jagathi, V., Anupama, B., Praveen, P.S. and Rao, G.D., 2010. Spectrophotometric determination of memantine in bulk and in pharmaceutical formulations. *Int J Curr Pharm Res*, **2**(4), 17-18 (2010).
  15. Atia, N.N., Marzouq, M.A., Hassan, A.I. and Eltoukhi, W.E., 2020. A rapid FTIR spectroscopic assay for quantitative determination of memantine hydrochloride and amisulpride in human plasma and pharmaceutical formulations. *Spectrochimica Acta Part A: Molecular and Biomolecular Spectroscopy*, **236**, 118377(2020).
  16. Reichová, N.A., Pazourek, J., Polášková, P. and Havel, J., Electrophoretic behavior of adamantane derivatives possessing antiviral activity and their determination by capillary zone electrophoresis with indirect detection. *Electrophoresis*, **23** (2), 259-262 (2002).
  17. Siddiqui, M.R.; Al-Othman, Z.A.; Rahman, N. Analytical techniques in pharmaceutical analysis: A review. *Arab. J. Chem.* 2017, **10**, S1409-S1421.
  18. Ozkan, S.A. Electroanalytical methods in pharmaceutical analysis and their validation. HNB publishing (2012).
  19. Ozkan, S.A.; Kauffmann, J.M.; Zuman, P. *Electroanalysis in biomedical and pharmaceutical sciences: voltammetry, amperometry, biosensors, applications*. Springer (2015).
  20. Ziyatdinova, G.; Budnikov, H. Electroanalysis of antioxidants in pharmaceutical dosage forms: state-of-the-art and perspectives. *Monatshefte Chem. Chem. Monthly*, **146**, 741-753 (2015).
  21. Bakker, E., Bühlmann, P and Pretsch, E., Polymer Membrane Ion-Selective Electrodes—What are the Limits?, *Electroanalysis*, **11**, 915-933(1999).
  22. K Gupta, V., Nayak, A., Agarwal, S. and Singhal, B., Recent advances on potentiometric membrane sensors for pharmaceutical analysis. *Combinatorial chemistry & high throughput screening*, **14**(4), 284-302 (2011).
  23. Özbek, O., Berkel, C. and Isildak, Ö., Applications of potentiometric sensors for the determination of drug molecules in biological samples. *Critical Reviews in Analytical Chemistry*, **52**(4), 768-779 (2022).
  24. Mostafa, I.M., Meng, C., Dong, Z., Lou, B. and Xu, G., Potentiometric sensors for the determination of pharmaceutical drugs. *Analytical Sciences*, **38** (1), 23-37 (2022).
  25. Isildak, Ö. and Özbek, O., Application of potentiometric sensors in real samples. *Critical Reviews in Analytical Chemistry*, **51** (3), 218-231 (2021).
  26. Metters, J.P., Kadara, R.O and Banks, C.E., New directions in screen printed electroanalytical sensors: an overview of recent developments. *Analyst*, **136**, 1067-1076 (2011).
  27. Metters, J.P., Randviir, E.P and Banks, C.E. Screen-printed back-to-back electroanalytical sensors. *Analyst*, **139**, 5339-5349. (2014)
  28. Hughes, G., Westmacott, K., Honeychurch, K.C., Crew, A.P., Pemberton, R and Hart, J.P., Recent advances in the fabrication and application of screen-printed electrochemical (bio) sensors based on carbon materials for biomedical, agri-food and environmental analyses. *Biosensors*, **6**, 50(2016).
  29. Mohamed, H.M., 2016. Screen-printed disposable electrodes: Pharmaceutical applications and recent developments. *TrAC*

- Trends in Analytical Chemistry*, **82**, 1-11 (2016).
30. Mostafa, I.M., Meng, C., Dong, Z., Lou, B. and Xu, G., Potentiometric sensors for the determination of pharmaceutical drugs. *Analytical Sciences*, **38**(1), 23-37 (2022).
  31. Özbek, O. and Altunoluk, O.C., Potentiometric determination of anti-epileptic drugs: A mini review. *Sensors International*, p.100224 (2022).
  32. Musa, A.M., Kiely, J., Luxton, R. and Honeychurch, K.C., Recent progress in screen-printed electrochemical sensors and biosensors for the detection of estrogens. *TrAC Trends in Analytical Chemistry*, **139**, 116254(2021).
  33. Ganjali, M.R., Aboufazeli, F., Riahi, S., Dinarvand, R., Norouzi, P., Ghasemi, M.H., Kiani-Anbuhi, R. and Meftah, S., Memantine potentiometric membrane sensor for memantine pharmaceutical analysis; computational investigation. *Int. J. Electrochem. Sci*, **4**, 1138-1152 (2009).
  34. Merey, H.A., Helmy, M.I., Tawakkol, S.M., Toubar, S.S. and Risk, M.S., Potentiometric membrane sensors for determination of memantine hydrochloride and pramipexole dihydrochloride monohydrate. *Portugaliae Electrochimica Acta*, **30**(1), 31-43 (2012).
  35. Alarfaj, N.A. and El-Tohamy, M.F., Conventional and Modified Nano Carbon Paste Sensors for Determination of Alzheimer's Drug Memantine Hydrochloride. *Sensor Letters*, **11**(10), 1968-1977 (2013).
  36. El Nashar, R.M., El-Tantawy, A.S. and Hassan, S.S., Potentiometric membrane sensors for the selective determination of memantine hydrochloride in pharmaceutical preparations. *Int. J. Electrochem. Sci*, **7**, 10802-10817 (2012).
  37. Hussien, E.M. and Derar, A.R., 3D spongy-like Au film for highly stable solid contact potentiometric ion selective electrode: Application to drug analysis. *SN Applied Sciences*, **1**, 1-11 (2019).
  38. Weber, E., *Supramolecular Chemistry II-Host Design and Molecular Recognition*, Springer-Verlag, Berlin Heidelberg, (1995).
  39. Ganjali, M.R., Norouzi, P., Rezapour, M., Faridbod, F., Pourjavid, M.R., Supramolecular based membrane sensors, *Sensors*, **6** (2006) 1018-1086.
  40. Shahgaldian, P. and Pieleś, U., Cyclodextrin derivatives as chiral supramolecular receptors for enantioselective sensing, *Sensors*, **6** 593-615(2006).
  41. Faridbod, F., Ganjali, M.R., Dinarvand, R., Norouzi, P. and Riahi, S., Schiff's bases and crown ethers as supramolecular sensing materials in the construction of potentiometric membrane sensors, *Sensors*, **8**, 1645-1073 (2008).
  42. Lenik, J., Cyclodextrins based electrochemical sensors for biomedical and pharmaceutical analysis. *Current Medicinal Chemistry*, **24**(22), 2359-2391 (2017).
  43. Yin, T. and Qin, W., Applications of nanomaterials in potentiometric sensors. *TrAC Trends in Analytical Chemistry*, **51**, 79-86 (2013).
  44. Brainina, K., Stozhko, N., Bukharinova, M. and Vikulova, E., Nanomaterials: Electrochemical properties and application in sensors. *Physical Sciences Reviews*, **3** (9) (2018).
  45. Ding, J. and Qin, W., Recent advances in potentiometric biosensors. *TrAC Trends in Analytical Chemistry*, **124**, p.115803 (2020).
  46. Manjunatha, C., Khosla, A., Krishna, R.H. and Ashoka, S., Current Progress in Materials, Device Fabrication, and Biomedical Applications of Potentiometric Sensor Devices: A Short Review. *ECS Transactions*, **107**(1), p.6343 (2022).
  47. Batten, S.R., Neville, S.M. and Turner, D.R. Porous coordination polymers, Chapter 10, in: *Coordination Polymers: Design*, The Royal Society of Chemistry, Cambridge, UK, pp. 313-344 (2009).
  48. Kumar, P., Deep, A. and Kim, K.H., Metal organic frameworks for sensing applications. *TrAC Trends in Analytical Chemistry*, **73**, pp.39-53 (2015).
  49. Wang, Z. and Cohen, S.M., Postsynthetic modification of metal-organic frameworks. *Chemical Society Reviews*, **38**(5), 1315-1329 (2009).
  50. Furukawa, H., Cordova, K.E., O'Keeffe, M. and Yaghi, O.M., The chemistry and applications of metal-organic frameworks. *Science*, **341**(6149), 1230444(2013).
  51. Zhu, Q.L. and Xu, Q., Metal-organic framework composites. *Chemical Society Reviews*, **43**(16), pp.5468-5512 (2014).
  52. Wang, S., Mc Guirk, C.M., d'Aquino, A., Mason, J.A. and Mirkin, C.A., Metal-organic framework nanoparticles. *Advanced Materials*, **30**(37), p.1800202 (2018).
  53. Hartlieb, K.J., Peters, A.W., Wang, T.C., Deria, P., Farha, O.K., Hupp, J.T. and

- Stoddart, J.F., Functionalized cyclodextrin-based metal-organic frameworks. *Chemical Communications*, **53**(54), 7561-7564 (2017).
54. He, Y., Hou, X., Liu, Y. and Feng, N., Recent progress in the synthesis, structural diversity and emerging applications of cyclodextrin-based metal-organic frameworks. *Journal of Materials Chemistry B*, **7**(37), 5602-5619 (2019).
55. Roy, I. and Stoddart, J.F., Cyclodextrin metal-organic frameworks and their applications. *Accounts of chemical research*, **54**(6), 1440-1453 (2021).
56. Dummert, S.V., Saini, H., Hussain, M.Z., Yadava, K., Jayaramulu, K., Casini, A. and Fischer, R.A., Cyclodextrin metal-organic frameworks and derivatives: recent developments and applications. *Chemical Society Reviews* (2022).
57. El-Attar, R.O., Abdelhameed, R.M., Khaled, E., Synthesis and applications of crown ether-linked metal organic framework composite based sensors for adsorptive differential pulse voltammetric determination of lead, *Arabian journal for science and engineering*, accepted(2023).
58. El-Attar, R.O., Abdelhameed, R.M., Khaled, E., Macromolecules cross linked-metal organic frameworks as a new candidate for Donepezil hydrochloride potentiometric sensors, *Electroanalysis*, under review (2023).
59. Khaled, E., Kamel, M.S., Hassan, H.N.A., Abdel-Gawad H and Aboul-Enein, H.Y., Performance of a portable biosensor for the analysis of ethion residues, *Talanta* **119**, 467-472 (2014).
60. Buck R. P. and Lindner, E., Recommendations for nomenclature of ion selective electrodes, *Pure Appl. Chem.* **66**, 2527-2536 (1994).
61. The United States Pharmacopoeia (USP 34). National Formulary (NF 29, 2011).
62. Jalalizadeh, H., Raei, M., FALLAH TAFTI, R., Farsam, H., Kebriaeezadeh, A. and Souri, E., A stability-indicating HPLC method for the determination of memantine hydrochloride in dosage forms through derivatization with 1-fluoro-2, 4-dinitrobenzene. *Scientia pharmaceutica*, **82**(2), 265-280 (2014).
63. Schaller, U., Bakker, E. and Pretsch, E.J., Carrier mechanism of acidic ionophores in solvent polymeric membrane ion-selective electrodes, *Anal. Chem.*, **67**, 3123-3132 (1995).
64. Schaller, U., Bakker, E., Spichiger, U.E. and Pretsch, E.J.A.C., Ionic additives for ion-selective electrodes based on electrically charged carriers, *Anal. Chem.* **66**, 391-398 (1994).
65. Bakker, E., Bühlmann P, and Pretsch, E., Polymer Membrane Ion-Selective Electrodes-What are the Limits?, *Electroanal.*, **11**, 915-933 (1999).
66. Vytras, K., Kalous J and Jezkova, J., Automated potentiometry as an ecologic alternative to two-phase titrations of surfactants, *Egypt. J. Anal. Chem.* **6**, 107-123 (1997).
67. Morf, W.J., The principles of ion-selective and of membrane transport, Elsevier, New York (1981).
68. Visser, H.C., De Jong F and Reinhoudt, D.N., Kinetics of carrier-mediated alkali cation transport through supported liquid membranes: Effect of membrane solvent, co-transported anion and support, *J. Membrane Sci.*, **107**, 267-276 (1995).
69. Umezawa, Y., CRC Handbook of ion-selective electrodes: selectivity coefficients, CRC press (1990).
70. Umezawa, Y., Bühlmann, P., Umezawa, K., Tohda K and Amemiya S., Potentiometric selectivity coefficients of ion-selective electrodes. Part I. Inorganic Cations, *Pure Appl. Chem.*, **72**, 1851-2082 (2002).
71. Tohda, K. Dragoe, D., Shibata M and Umezawa, Y., Studies on the matched potential method for determining the selectivity coefficients of ion-selective electrodes based on neutral ionophores: experimental and theoretical verification, *Anal. Sci.*, **17**, 733-743 (2001).
72. Guidance for Industry, 3QB (R2) Impurities in New Drug Products, U.S. Food and Drug Administration, Rockville, Md, USA, ICH Revision 2, 2006
73. Görög, S. Critical review of reports on impurity and degradation product profiling in the last decade. *TrAC Trends Anal. Chem.* **101**, 2-16 (2018).
74. Olsen, B.A and Baertschi, S.W, Strategies for investigation and control of process- and degradation-related impurities. In *Separation Science and Technology* **5**, 89-117 Academic Press, 2004.
75. Jain, D and Basniwal, P.K., Forced degradation and impurity profiling: recent trends in analytical perspectives. *J. Pharmaceut. Biomed. Anal.* **86**, 11-35 (2013).



76. Moffat, A.C., Osselten, M.D and Widdop, B., Clarke's Analysis of Drugs and Poisons in Pharmaceuticals, Body Fluids and Postmortem Material, 3rd Ed., Pharmaceutical Press, London, UK, 2004, 1370.
77. Vytras K., Potentiometric titrations based on ion- pair formation. *Ion Select. Electrode Rev.*, **7**, 77- 164 (1985).
78. Van Marum RJ. Update on the use of memantine in Alzheimer's disease. *Neuropsychiatr Dis Treat.* **5**, 237-47 (2009).
79. Bohets, H.Vanhoutte, K. De Maesschalck, R. Cockaerts, P.Vissers, B and Nagels, L., J. Development of in situ ion selective sensors for dissolution. *Anal. Chim. Acta*, **581** (1), 181–191 (2007).
80. Khaled, E., El-Sabbagh, I.A., El-Kholy, N.G. and Ghahni, E.A., Novel PVC-membrane electrode for flow injection potentiometric determination of Biperiden in pharmaceutical preparations. *Talanta*, **87**, 40-45 (2011).
81. Elzanfaly, E.S., Hassan, S.A. Salem, M.Y and El-Zeany, B.A., In-line potentiometric monitoring of dissolution behavior of verapamil hydrochloride versus traditional pharmacopeial method: A comparative study. *Sensors Actuators, B Chem.* **228**, 587–594 (2016).